Inorganics **2015**, *3*, 355-369; doi:10.3390/inorganics3030355

OPEN ACCESS

inorganics

ISSN 2304-6740

www.mdpi.com/journal/inorganics

Article

Vanadium(V)-Substitution Reactions of Wells–Dawson-Type Polyoxometalates: From $[X_2M_{18}O_{62}]^{6-}$ (X = P, As; M = Mo, W) to $[X_2VM_{17}O_{62}]^{7-}$

Tadaharu Ueda *, Yuriko Nishimoto, Rie Saito, Miho Ohnishi and Jun-ichi Nambu

Department of Applied Science, Faculty of Science, Kochi University, Kochi 780-8520, Japan

* Author to whom correspondence should be addressed; E-Mail: chuji@kochi-u.ac.jp; Tel.: +81-88-844-8299; Fax: +81-88-844-8359.

Academic Editors: Greta Ricarda Patzke and Pierre-Emmanuel Car

Received: 14 April 2015 / Accepted: 25 June 2015 / Published: 14 July 2015

Abstract: The formation processes of V(V)-substituted polyoxometalates with the Wells–Dawson-type structure were studied by cyclic voltammetry and by ^{31}P NMR and Raman spectroscopy. Generally, the vanadium-substituted heteropolytungstates, $[P_2VW_{17}O_{62}]^{7-}$ and $[As_2VW_{17}O_{62}]^{7-}$, were prepared by mixing equimolar amounts of the corresponding lacunary species—$[P_2W_{17}O_{61}]^{10-}$ and $[As_2W_{17}O_{61}]^{10-}$—and vanadate. According to the results of various measurements in the present study, the tungsten site in the framework of $[P_2W_{18}O_{62}]^{6-}$ and $[As_2W_{18}O_{62}]^{6-}$ without defect sites could be substituted with V(V) to form the $[P_2VW_{17}O_{62}]^{7-}$ and $[As_2VW_{17}O_{62}]^{7-}$, respectively. The order in which the reagents were mixed was observed to be the key factor for the formation of Dawson-type V(V)-substituted polyoxometalates. Even when the concentration of each reagent was identical, the final products differed depending on the order of their addition to the reaction mixture. Unlike Wells–Dawson-type heteropolytungstates, the molybdenum sites in the framework of $[P_2Mo_{18}O_{62}]^{6-}$ and $[As_2Mo_{18}O_{62}]^{6-}$ were substituted with V(V), but formed Keggin-type $[PVMo_{11}O_{40}]^{4-}$ and $[AsVMo_{11}O_{40}]^{4-}$ instead of $[P_2VMo_{17}O_{62}]^{7-}$ and $[As_2VMo_{17}O_{62}]^{7-}$, respectively, even though a variety of reaction conditions were used. The formation constant of the $[PVMo_{11}O_{40}]^{4-}$ and $[AsVMo_{11}O_{40}]^{4-}$ was hypothesized to be substantially greater than that of the $[P_2VMo_{17}O_{62}]^{7-}$ and $[As_2VMo_{17}O_{62}]^{7-}$.

Keyword: polyoxometalate; Wells–Dawson; vanadium; substitution

1. Introduction

Metal-substituted or metal-incorporated polyoxometalates (POMs) based on the Keggin and Wells–Dawson structures are of great interest in catalysis and other applications, as well as in fundamental studies, because they exhibit specific and excellent properties depending on the incorporated metals [1–9]. Cobalt- and ruthenium-incorporated POMs, such as $[Co_4(H_2O)_2(XW_9O_{34})_2]^{n-}$ (X = P, Si) and $Rb_8K_2[\{Ru_4O_4(OH)_2(H_2O)_4\}\text{-}(\gamma\text{-}SiW_{10}O_{36})_2]$, in particular, exhibit excellent catalytic activity toward water oxidation and water splitting [10–15]. Among the various metal-substituted POMs, vanadium-substituted POMs have been extensively investigated in terms of synthesis, characterization and applications. In particular, they have been used as oxidation catalysts in various organic syntheses, because they can be reduced at a more positive potential than the corresponding parent, non-substituted POMs [16–26]. Interestingly, vanadate can also be incorporated as the central ion of POMs [27–32]. Generally, metal-substituted or metal-incorporated POMs have been prepared with transition-metal atoms incorporated into the vacant sites of the lacunary species, such as $[PW_{11}O_{39}]^{7-}$ and $[P_2W_{17}O_{61}]^{10-}$ [1–9]. A variety of Wells–Dawson-type molybdenum- and/or vanadium-substituted tungstophosphates have been prepared from the parent $[P_2W_{18}O_{62}]^{6-}$ via a decomposition and re-building method by controlling the pH (Figure 1). Large-sized POMs have also been prepared by mixing metal cations and the lacunary POMs as building blocks. Currently, the synthesis of metal-substituted or metal-incorporated POMs can be controlled to some extent through the use of the lacunary POMs. In addition, details of the formation of some of POMs have been investigated using NMR and Raman spectroscopy and cyclic voltammetry [33–43]. However, many aspects of the formation of POMs in solution remain ambiguous.

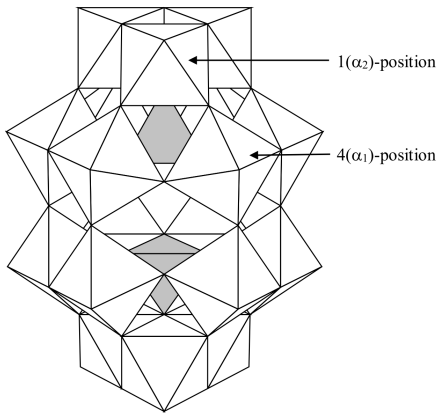

Figure 1. Structure of the Well–Dawson-type polyoxometalate.

Recently, we investigated the formation of Keggin-type V(V)-substituted POMs, $[XV_aM_{12-a}O_{40}]^{(3+a)-}$ (X = P, As, Si, Ge; M = Mo, W; a = 1, 2) (XV_aM_{12-a}), in both aqueous and aqueous-organic solutions using cyclic voltammetry, Raman spectroscopy and ^{31}P NMR [44,45]. Unlike other metal-substituted POMs, vanadate ions could be substituted, along with a few molybdenum or tungsten units, into the framework of XM_{12}, which did not contain vacant sites, to form V(V)-substituted POMs. On the basis

of this idea, mono-vanadium-substituted tungstosulfates 1- and 4-$[S_2VW_{17}O_{62}]^{5-}$ (S_2VW_{17}) were prepared by substituting vanadate for tungsten units in the framework of $[S_2W_{18}O_{62}]^{4-}$ (S_2W_{18}) [46].

In the present study, we investigated the formation of Wells–Dawson-type vanadium-substituted POMs, $[X_2VM_{17}O_{62}]^{7-}$ (X_2VM_{17}) (X = As, P; M = Mo, W) from the parent POMs, $[X_2M_{18}O_{62}]^{6-}$ (X_2M_{18}) using ^{31}P NMR and Raman spectroscopy and cyclic voltammetry.

2. Results and Discussion

2.1. Characterization of POMs Related to the Present Study

Solid-state Raman bands of all of the investigated POMs and the ^{31}P NMR signals of P_2W_{18}, P_2VW_{17}, P_2Mo_{18} and related phosphorus-containing POMs are listed in Tables 1 and 2, respectively. Characteristic bands and signals were used to assign peaks observed in the spectra of the products of the vanadium-substitution reaction in the solution phase.

Table 1. Raman band (cm^{-1}) of As_2VW_{17}, As_2W_{18}, P_2VW_{17}, P_2W_{18}, P_2Mo_{18} and As_2Mo_{18}.

Compounds	ν_{Raman}(M-O_d)
As_2VW_{17}	982
As_2W_{18}	982 (995) [a]
P_2VW_{17}	985
P_2W_{18}	983 (993) [a]
P_2Mo_{18} [b]	971
As_2Mo_{18} [b]	971

O_a: oxygen bonded with arsenic atom; O_b: octahedral corner-sharing oxygen; O_c: octahedral edge-sharing oxygen; O_d: terminal oxygen; M: W or Mo; X: P or As. The counter cation is *n*-Bu_4N^+. [a,b] Raman band of $K_6As_2W_{18}O_{62}$ and $K_6P_2W_{18}O_{62}$ from [47,48], respectively.

Table 2. ^{31}P NMR signal of phosphorus-centered polyoxometalates (POMs).

Compounds	^{31}P NMR signals (vs 85% H_3PO_4)	Ref.
α-P_2W_{18}	−12.44	[49]
β-P_2W_{18}	−11.0, −11.7	[50]
1-P_2W_{17}	−6.79, −13.63	[49]
4-P_2W_{17}	−8.53, −12.86	[49]
P_2W_{15}	+0.1, −13.3	[50]
1-P_2VW_{17}	−10.84, −12.92	[49]
4-P_2VW_{17}	−11.83, −12.90	[49]
1,2,3-$P_2V_3W_{15}$	−6.25, −13.89	[49]
α-PW_{12}	−14.42	[45]
β-PW_{12}	−13.50	[45]
PW_{11}	−11.8 [a], −10.2 [b]	[41]
A-α-PW_9	−5.1	[41]
PVW_{11}	−14.11	[45]
P_2Mo_{18}	−2.45	[47]
α-PMo_{12}	−3.16	[47]
PMo_{11}	−0.79 [c], −1.05 [d]	[51]
A-PMo_9	−0.93	[47]
$PVMo_{11}$	−3.53	[44]

[a] Measured at pH 2.0; [b] measured at pH 4.0-7.5; [c] measured at pH 3.4; [d] measured at pH 2.5.

The major Raman lines of the As_2W_{18} and As_2VW_{17} complexes were observed at 995 and 982 cm^{-1}, respectively. The Raman band at approximately 990 cm^{-1} is due to the stretching mode of W-O_d and is affected by the cation in the solid state [52]. The Raman bands of the *n*-Bu_4N^+ salts of As_2W_{18} and P_2W_{18}, in which a small number of H^+ are included as counter cations, occur at lower wavenumbers than those of small cation salts, such as potassium. These Raman bands were used as reference signals to investigate the formation and conversion processes of the As_2W_{18} and As_2VW_{17} complexes in the reaction mixtures, while taking into consideration the effect of the proton.

Cyclic voltammograms of 5.0×10^{-4} M $X_2V_aW_{18-a}$ (X = P, As; a = 0, 1) were measured in 95% (*v*/*v*) CH_3CN containing 0.1 M $HClO_4$ (Figure A1). Details are provided in the Supporting Information. The voltammetric behaviors of X_2VW_{17} were used to determine whether the vanadium-substitution reaction occurred on the basis of the appearance of a new redox wave at a more positive potential than that of the corresponding parent non-substituted species.

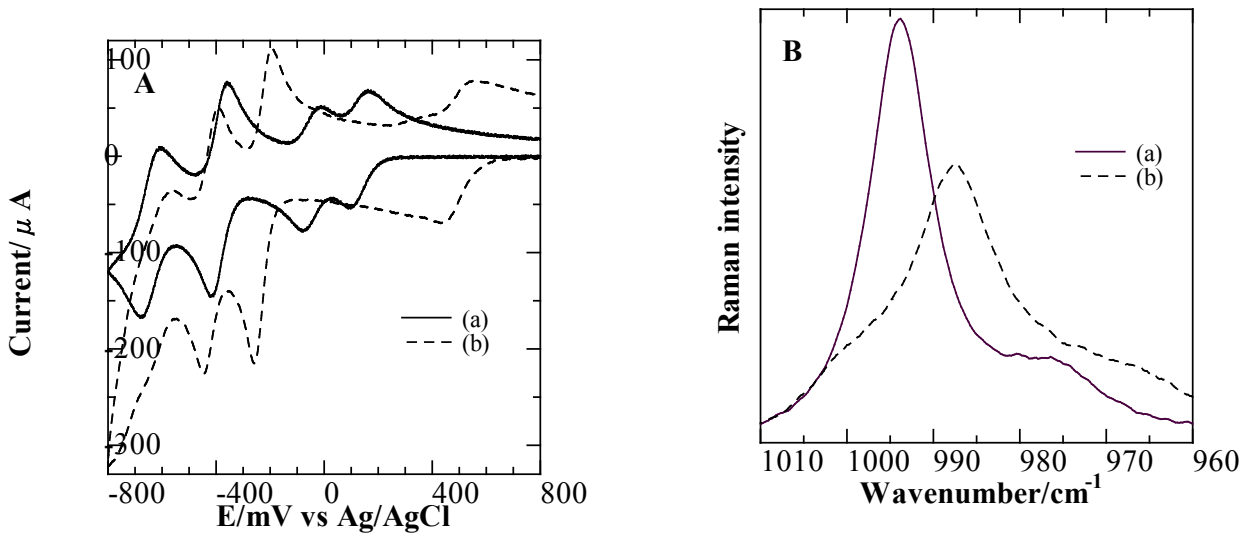

Figure 2. Cyclic voltammograms (**A**) and Raman spectra (**B**) of a 100 mM W(VI)–200 mM As(V)–10 mM V(V)–pH 2.0 system collected (a) after a solution without V(V) was heated at 80 °C for one week and (b) after 10 mM V(V) was added and the solution was heated again at 80 °C for one day.

2.2. Formation of Dawson-Type Vanadium-Substituted Tungstoarsenate and Tungstophosphate Complexes

Figures 2A(a) and 2B(a) show a cyclic voltammogram and a Raman spectrum, respectively, of a 100 mM W(VI)–200 mM As(V)–pH 2.5 system heated at 80 °C for one week. Four-step reduction waves were observed at 95, −83, −416 and −676 mV, which corresponded to one-, one-, two- and two-electron transfers, respectively. In addition, a Raman peak appeared at 994 cm^{-1}. These voltammetric waves and the Raman peak are due to the formation of the As_2W_{18}. After 10 mM V(V) was added, the pH was re-adjusted to 2.5 with conc. HCl and the solution was heated at 80 °C for one day; the original reduction waves and the Raman peak at 994 cm^{-1} disappeared, and new reduction waves at 437, −263 and −448 (Figure 2A(b)) and a new Raman band at 988 cm^{-1} appeared (Figure 2B(b)). The voltammetric and Raman spectral behaviors indicate that one of the tungsten units in the As_2W_{18} was substituted with

vanadate to form the As_2VW_{17}. The vanadium substitution of P_2W_{18} leads to 1-P_2VW_{17}, whose vanadium is located at a polar site, as described below. In addition, the Wells–Dawson-type 1-S_2VW_{17} was prepared by addition of V(V) to the reaction mixture, where the parent S_2W_{18} is dominant [46]. The vanadium unit of the observed As_2VW_{17} was located at the polar position, although Raman spectroscopy, cyclic voltammetry and other measurements provided no information on this perspective.

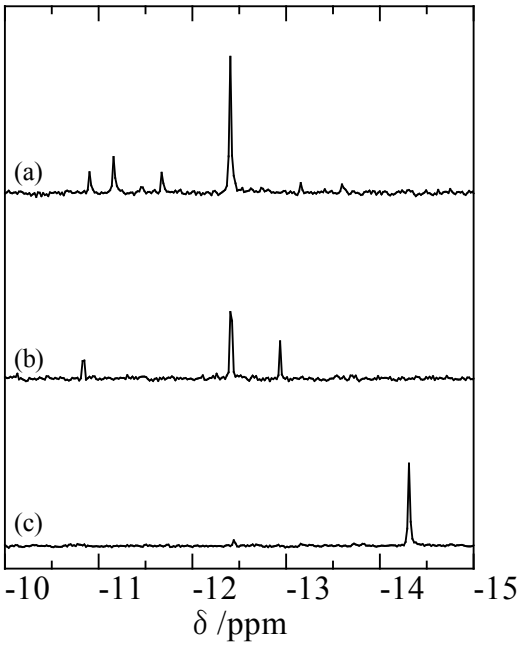

Figure 3. ^{31}P NMR spectrum of a 100 mM W(VI)–500 mM P(V)–V(V)–pH 2.0 system collected (**a**) after a solution without V(V) was heated at 80 °C for one week, (**b**) after 50 mM V(V) was added and the solution was heated again at 80 °C for one day and (**c**) after a solution of 100 mM W(VI)–500 mM P(V)–50 mM V(V)–pH 2 was heated at 80 °C for one week.

The formation of P_2VW_{17} by the substitution reaction of P_2W_{18} with V(V) was investigated using ^{31}P NMR. After a solution of 100 mM W(VI) and 500 mM P(V) was heated at pH 2 at 80 °C for one week, four main ^{31}P NMR peaks at −10.9, −11.2, −11.7 and −12.4 ppm were observed; these peaks were attributed to the formation of α-P_2W_{18} (−12.4 ppm), β-P_2W_{18} (−10.9, −11.7 ppm) and PW_{11} (−11.2 ppm) (Figure 3a). Upon further heating at 80 °C for one day following the addition of 50 mM V(V) and adjustment of the pH to 2.0, the three peaks at –10.9, −11.2 and −11.7 ppm disappeared, whereas two new peaks appeared at –10.8 and –12.9 ppm; these peaks were ascribed to the formation of the 1-P_2VW_{17}. However, the peak at –12.4 ppm did not completely disappear despite the addition of 100 mM V(V). A similar result was obtained in the case of the substitution reaction of the Keggin-type XM_{12} (X = P, As; M = Mo, W) with V(V). The PW_{12} and PMo_{12} were not fully converted into PV_aW_{12-a} and PV_aMo_{12-a}, respectively, in aqueous CH_3CN solution, although both AsW_{12} and $AsMo_{12}$ were fully converted into the corresponding vanadium-substituted species [44,45]. The relatively high stability of P_2W_{18}, compared to that of As_2W_{18} would lead to incomplete conversion of the P_2W_{18} into the P_2VW_{17}, similar to the conversion of the PM_{12} (M = Mo, W) into the PVM_{11}.

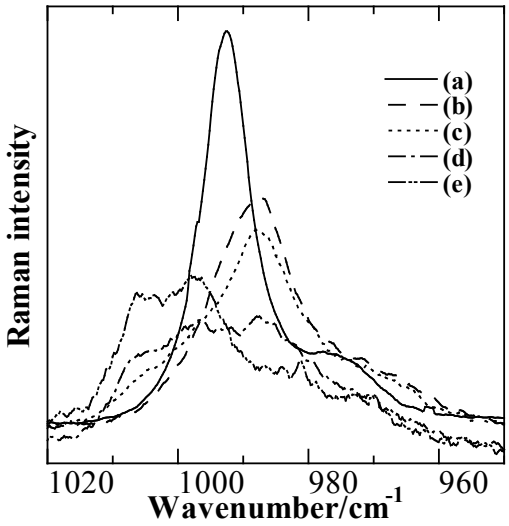

Figure 4. Raman spectra of a 100 mM W(VI)–200 mM As(V)–pH 2.0 system containing various concentrations of V(V) collected after each solution was heated at 80 °C for one week. [V(V)]/mM = (a) 0; (b) 5; (c) 10; (d) 15; and (e) 20.

To investigate the direct formation of X_2VW_{17} (X = As, P), but not through X_2W_{18} as an intermediate species, Raman spectra and ^{31}P NMR spectra were collected after a solution of W(VI)–V(V)-As(V) or –P(V) was heated at an appropriate pH. Figure 4 shows the Raman spectra collected after a solution of 100 mM W(VI), 200 mM As(V) and 0–20 mM V(V) were heated at pH 2 at 80 °C for one week. In the presence of 5–15 mM V(V), the Raman peak shifted from 993 cm^{-1} to 987 cm^{-1} when the concentration of V(V) was increased, thereby indicating the substitution of a tungsten unit in As_2W_{18} with V(V) to form As_2VW_{17}. However, a broad, new Raman peak appeared at 1005 cm^{-1}, and its intensity increased depending on the concentration of V(V) (7–20 mM) (Figure 4, (d) and (e)). The new peak at approximately 1005 cm^{-1} was due to the formation of Keggin-type $AsVW_{11}$ [45]. Indeed, $AsVW_{11}$ was isolated along with As_2VW_{17} when prepared in accordance with the literature [48], where the solution conditions used in the synthesis were similar to those used in our experiments, as previously described.

Figure 3c shows the ^{31}P NMR spectrum collected for a solution of 100 mM W(VI), 500 mM P(V) and 50 mM V(V) at pH 2 heated at 80 °C for one week. Only one peak (at –14.3 ppm) was observed that was attributable to the formation of the Keggin-type PVW_{11}. Even when the concentration of V(V) was increased or decreased, the two peaks at –10.8 and –12.9 ppm associated with the formation of P_2VW_{17} were not observed. Notably, the occurrence of As_2W_{18} or P_2W_{18} in the reaction mixture appears to be essential for the formation of the corresponding V(V)-substituted species, As_2VW_{17} and P_2VW_{17}.

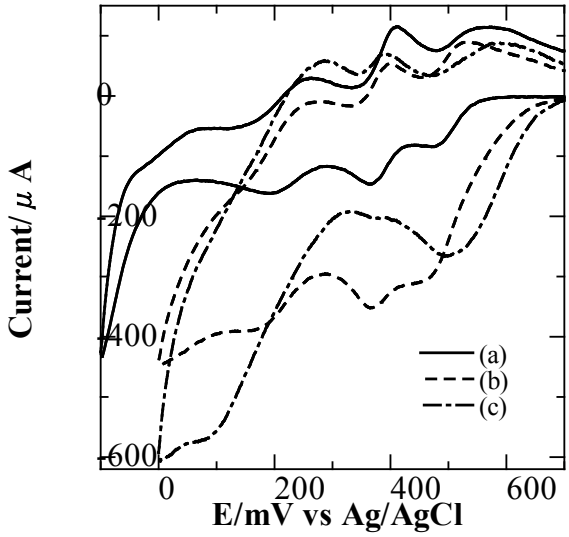

Figure 5. Cyclic voltammograms of a 100 mM Mo(VI)–10 mM As(V)–10 mM V(V)–0.5 M HCl system collected (a) after a solution without V(V) was heated at 80 °C for 7 h, (b) immediately after 10 mM V(V) was added to solution (a) and subsequently heated at 80 °C for 2 h and (c) after solution (b) was heated at 80 °C for one day.

2.3. Formation of Wells–Dawson-Type Vanadium-Substituted Molybdoarsenate and Molybdophosphate Complexes

The vanadium substitution reactions of P_2Mo_{18} and As_2Mo_{18} were also investigated using cyclic voltammetry and ^{31}P NMR spectroscopy. Three reduction peaks appeared at 477, 363 and 194 mV in the cyclic voltammogram collected after a solution of 100 mM Mo(VI), 10 mM As(V) and 0.5 M HCl was heated at 80 °C for 8 h; these peaks were due to the formation of As_2Mo_{18} (Figure 5(a)) [47]. After 10 mM V(V) was added and the solution was heated at 80 °C for 2 h, the original three peaks increased in magnitude of current, but the reduction potentials did not change (Figure 5(b)). Moreover, after the solution was heated at 80 °C for 15 h, a new reduction peak appeared at 500 mV in addition to a small peak at 375 mV, whereas the intensities of the original three reduction waves were diminished (Figure 5(c)). This new wave is ascribed to the formation of Keggin-type AsV_aMo_{12-a} [44]. In fact, only AsV_zMo_{12-z} (z = 1,2) could be isolated as a tetra-alkyl ammonium salt from this solution (see the Supporting Information). The occurrence of $AsVMo_{17}$ has not been confirmed, although we have extensively examined the solution under various conditions. In addition, we have investigated the direct formation of As_2VMo_{17} from a Mo(VI)–As(V)–V(V)–HCl system under various conditions. However, only Keggin-type vanadium-substituted molybdoarsenate was formed in the solution.

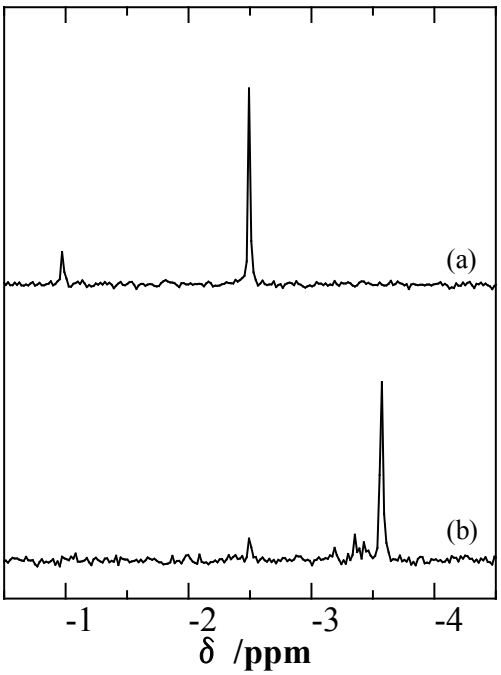

Figure 6. ^{31}P NMR spectra of a 100 mM Mo(VI)–100 mM P(V)–25 mM V(V)–1.0 M HCl system collected (**a**) after a solution without V(V) was heated at 80 °C for 30 h and (**b**) after V(V) was added and the solution was heated again at 80 °C for one day.

The substitution reaction of a molybdenum unit in P_2Mo_{18} with V(V) into P_2VMo_{17} was also extensively investigated. The ^{31}P NMR spectrum for a 100 mM Mo(VI)–100 mM P(V)–1.0 M HCl system showed two peaks at −0.97 and −2.49 ppm due to the formation of PMo_9 and P_2Mo_{18}, respectively (Figure 6a) [33,34,47]. After 10 mM V(V) was added and the solution was allowed to stand at room temperature for 1 h, new peaks appeared at −3.57 in addition several peaks at around −3.4 ppm, which are ascribed to the formation of mono-vanadium-substituted and multi-vanadium-substituted Keggin-type molybdophosphate, respectively. Meanwhile, the intensities of the peaks at −0.97 ppm and −2.49 ppm decreased in intensity, indicating that a small amount of P_2Mo_{18} remained in the solution. Although we have investigated the solutions under various conditions by changing the order of addition of reagents and the heating time, only Keggin-type vanadium-substituted molybdophosphates were formed. As with the Mo(VI)–As(V)–V(V) system, no P_2VMo_{17} appeared at any considerable concentration in the Mo(VI)–P(V)–V(V) system. For both the Mo(VI)–V(V)–As(V) and –P(V) systems, no X_2VMo_{17}(X = As, P) formed from X_2Mo_{18}. These results suggest that Keggin-type $XVMo_{11}$ should be substantially more stable than Wells–Dawson-type X_2VMo_{17} in the solution.

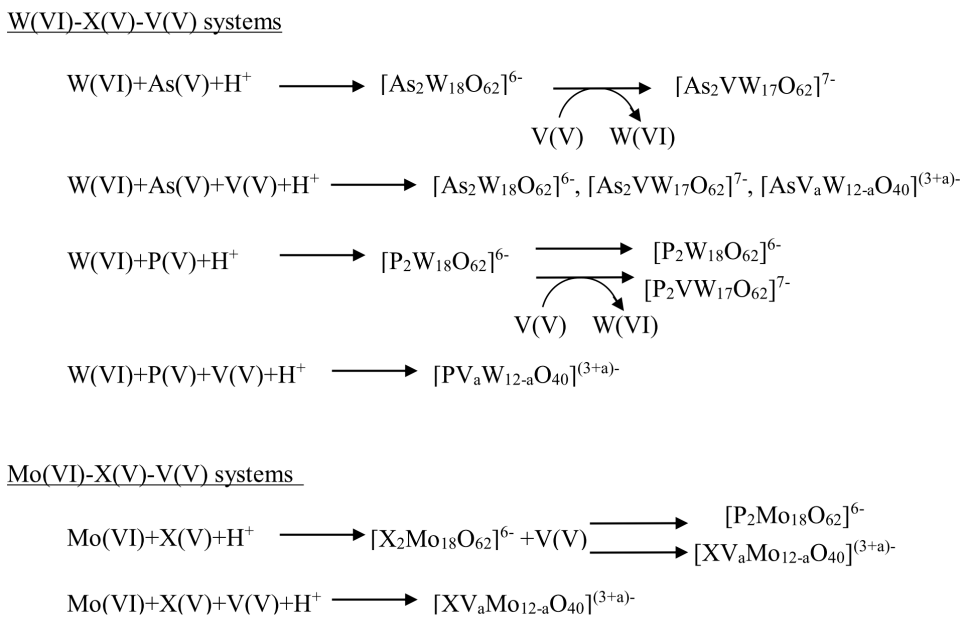

Scheme 1. Vanadium substitution reaction of Wells–Dawson-type POMs for the M(VI)–X(V)–V(V) (M = W, Mo; X = P, As) systems in aqueous solution.

3. Experimental Section

Voltammetric measurements were performed using a microcomputer-controlled system. A glassy carbon (GC) electrode (BAS GC-30S) with a surface area of 0.071 cm^2 was used as the working electrode, and a platinum wire served as the counter electrode. The reference electrodes were Ag/AgCl (saturated KCl) for aqueous solutions and Ag/Ag^+ (0.01 M (M = mol/dm^3) $AgNO_3$ in acetonitrile) for acetonitrile solutions. Prior to each measurement, the GC electrode was polished with 0.1-μm diamond slurry and washed with distilled water. The voltammograms were recorded at 25 ± 0.1 °C. Unless otherwise noted, the voltage scan rate was 100 mV/s. Raman spectra were recorded on a Horiba Jobin Yvon model HR-800 spectrophotometer. The argon line at 514.5 nm was used for excitation. The Raman measurements were conducted at 20 °C. For quantitative measurements, the Raman intensities were normalized by the 1048-cm^{-1} band associated with NO_3^-; 0.1 M $NaNO_3$ was added and used as an internal standard. The ^{31}P NMR measurements were performed on a JEOL model JNM-LA400 spectrometer at 161.70 MHz. An inner tube containing D_2O was used as an instrumental lock. Chemical shifts were referenced to 85% H_3PO_4. The preparation procedures of the *n*-Bu_4N^+ salts of the POMs used in the present study are described in the Appendix.

4. Conclusions

In the present study, the V(V)-substitution reactions of Wells–Dawson-type POMs were investigated in aqueous solution using ^{31}P NMR and Raman spectroscopy and cyclic voltammetry. The elucidated vanadium substitution reaction processes are summarized in Scheme 1. The addition of V(V) ions to a solution containing As_2W_{18} or P_2W_{18} led to the corresponding As_2VW_{17} or 1-P_2VW_{17}, respectively, although not all P_2W_{18} in the solution was completely transformed into 1-P_2VW_{17}, even after a large excess of V(V) was added. These results suggest that P_2W_{18} is more stable than As_2W_{18}. As_2VW_{17} and 1-P_2VW_{17} can be prepared directly from As_2W_{18} and P_2W_{18}, respectively, via the addition of V(V), a

synthetic procedure that is simpler than those previously reported [48–51]. This simplified procedure enables the preparation of a large amount of X_2VW_{17} at industrial levels as oxidant catalysts at low cost. Interestingly, tungsten in the one-position of X_2W_{18} could be substituted with V(V) to form X_2W_{17}, while X_2W_{18} decomposed with a weak base to form 4-X_2W_{17}. The order of addition of the reagents to the reaction mixture was very important. Even when the concentrations of W(VI), V(V), H^+ and P(V) or As(V) were the same, mixing and then heating the reagents led to the Keggin-type XVW_{11}, although As_2VW_{17} was observed as a mixture in the case of the As(V) system. This result implies that the occurrence of X_2W_{18} in the reaction mixtures was essential for the formation of the corresponding V(V)-substituted species, X_2VW_{17}. In contrast, only $XVMo_{11}$ (X = As, P) formed, rather than X_2VMo_{17}, in the Mo(VI)–V(V)–P(V) and –As(V) systems, even when various concentrations of V(V), P(V), As(V) and acid were used and the order of the addition of the reagents was varied. The results suggested that the formation constants of $XVMo_{11}$ are likely much greater than those of X_2VMo_{17}. To the best of our knowledge, the literature contains few reports of the synthesis of Wells–Dawson-type vanadium-substituted phosphorus- and arsenic-centered heteropolymolybdates, X_2VMo_{17} (X = P, As). According to the results of the present study, X_2VMo_{17} cannot be synthesized using simple procedures.

Acknowledgements

This work was supported by a Grant-in-aid for Scientific Research (No. 25410095) from the Ministry of Education, Culture, Sports, Science and Technology of Japan, a Special Research Grant for Rare Metals and Green Technology and a Kochi University President's Discretionary Grant.

Author Contributions

T.U.: Writing the manuscript and discussion of the results; Y.N. and R.S.: voltammetry and Raman spectroscopy measurements; M.O. and J.N.: Synthesis of polyoxometalates and ^{31}P NMR spectroscopy measurement.

Conflicts of Interest

The authors declare no conflict of interest.

Appendix

A1. Cyclic Voltammograms of $X_2V_aW_{18-a}$ (X = P, As; a = 0, 1)

Figure A1 shows the cyclic voltammograms of 5.0×10^{-4} M $X_2V_aW_{18-a}$ (X = P, As; a = 0, 1) in 95% (*v*/*v*) CH_3CN containing 0.1 M $HClO_4$. The X_2W_{18} complexes exhibit two-step redox waves with midpoint-potentials (E_{mid}) of -440 and -610 mV *vs.* Fc/Fc^+ for P_2W_{18} and -400 and -550 mV for As_2W_{18}, with a current ratio of 1:1, where $E_{mid} = (E_{pc} + E_{pa})/2$, where E_{pc} is the cathodic peak potential and E_{pa} is the anodic peak potential. Each wave was diffusion-controlled. Coulometric analysis and normal-pulse voltammetric measurements confirmed that the two-step reduction waves corresponded to two two-electron transfers. In the case of cyclic voltammetry performed in aqueous acid solution (pH = 1.0: [HCl] = 0.1 M and [NaCl] = 0.9 M), the first two-electron transfer redox wave observed in Fig. 2 was

split into two one-electron transfer waves at +0.04 and −0.14 V *vs.* SCE for P_2W_{18}, and +0.08 and -0.10 V for As_2W_{18} [53,54]. Because the redox potential of the vanadium components of vanadium-substituted POMs XVM_{11} and S_2VW_{17} was more positive than those of the molybdenum or tungsten components in these complexes, the reduction waves at approximately 200 mV should be ascribed to the reduction of V(V) to V(IV) in the X_2VW_{17} complexes [46,55–58]. Each of the E_{mid} for PM_{12} (M = Mo, W) occurred at a more negative potential than that of the corresponding AsM_{12}. Similarly, each E_{mid} for P_2W_{18} and P_2VW_{17} also occurred at a more negative potential than that of the corresponding As_2W_{18} and As_2VW_{17}, although we could not elucidate the origin of the oxidation wave at 0 mV in the voltammograms of As_2VW_{17} and P_2VW_{17}. No oxidation wave was observed when the switch potential was set at a more positive potential than the tungsten reduction potential. On the basis of these voltammetry results, the occurrence of the vanadium substitution reaction can be determined from the appearance of a new peak at more positive potentials than the redox potentials of the Mo or W component in the POMs after the addition of V(V) to the reaction mixtures.

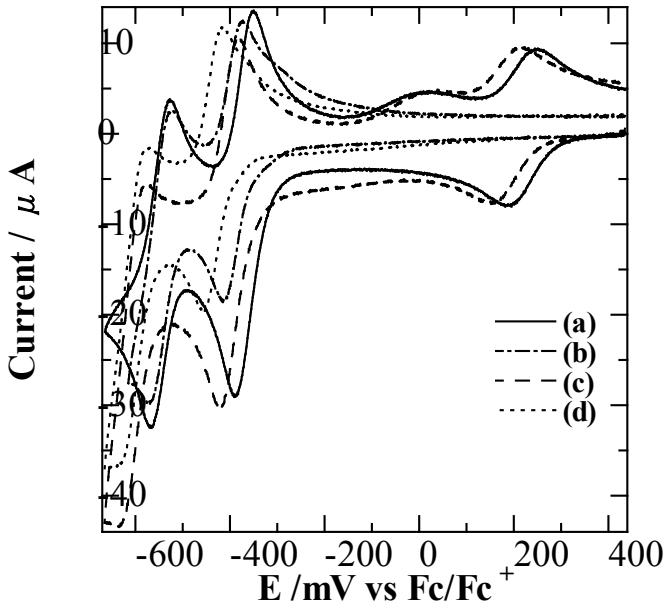

Figure A1. Cyclic voltammograms of (a) $[As_2VW_{17}O_{62}]^{7-}$, (b) $[As_2W_{18}O_{62}]^{6-}$, (c) $[P_2VW_{17}O_{62}]^{7-}$, and (d) $[P_2W_{18}O_{62}]^{6-}$ in 95% (v/v) CH_3CN containing 0.1 M $HClO_4$.

A2. Identification of POMs Isolated as a *tetra*-Butylammonium Salt from a 100 mM Mo(VI)–10 mM As(V)–0.5 M HCl System after the Addition of 5–20 mM V(V)

POMs were isolated as a tetra-butylammonium salt from a 100 mM Mo(VI)–10 mM As(V)–0.5 M HCl–5–20 mM V(V) system after measuring cyclic voltammograms as shown in Figure 5. The IR spectra of the isolated salts were measured using a Jasco 460-plus IR spectrometer; IR bands were observed at 950, 890, 847, and 786 cm^{-1}. These bands were compared with the reported data to identify the mixture of n-Bu_4N^+ salts of $[AsVMo_{11}O_{40}]^{4-}$ and $[AsV_2Mo_{10}O_{40}]^{5-}$ [44].

References

1. Pope, M.T. *Heteropoly and Isopoly Oxometalates*; Springer: Berlin, Gemany, 1983.
2. Hill, C.L. Introduction: Polyoxometalates s Multicomponent Molecular Vehicles To Probe Fundamental Issues and Practical Problems. *Chem. Rev.* **1998**, *98*, 1-390.
3. Pope, M.T.; Müller, A. *Polyoxometalate Chemistry From Topology via Self-Assembly to Applications*; Kluwer Academic Publishers: New York, NY, USA, 2001.
4. Yamase, T.; Pope, M.T. Eds., *Polyoxometalate Chemistry for Nano-Composite Design*, Kluwer Academic/Plenum Publishers: New York, NY, USA, 2002.
5. Borrás-Almenar, J.J.; Coronado, E.; Müller, A.; Pope, M.T. *Polyoxometalate Molecular Science*; Kluwer Academic Publishers: New York, NY, USA, 2003.
6. Mialane, P.; Dolbecq, A.; Sécheresse, F. Functionalization of polyoxometalates by carboxylato and azido ligands: macromolecular complexes and extended compounds. *Chem. Commun.* **2006**, *33*, 3477–3485.
7. Long, D.-L.; Burkholder, E.; Cronin, L. Polyoxometalate clusters, nanostructures and materials: From self assembly to designer materials and devices. *Chem. Soc. Rev.* **2007**, *36*, 105–121.
8. Proust, A.; Thouvenot, R.; Gouzerh, P. Functionalization of polyoxometalates: towards advanced applications in catalysis and materials science, *Chem. Commun.* **2008**, 1837–1852
9. Ueda, T.; Kotsuki, H. Heteropoly acids: green chemical catalysts in organic synthesis, *Heterocycle* **2008**, *76*, 73–97.
10. Huang, Z.; Luo, Z.; Geletii, Y.V.; Vickers, J.W.; Yin, Q.; Wu, D.; Hou, Y.; Ding, Y.; Song, J.; Musaev, D.G.; Hill, C.L.; Lian, T. Efficient light-driven carbon-free cobalt-based molecular catalyst for water oxidation, *J. Am. Chem. Soc.* **2011**, *133*, 2068–2071.
11. Car, P.-E.; Guttentag, M.; Baldridge, K.K.; Alberto, R.; Patzke, G.R. Synthesis and characterization of open and sandwich-type polyoxometalates reveals visible-light-driven water oxidation via POM-photosensitizer complexes, *Green Chem.* **2012**, *14*, 1680–1688.
12. Natali, M.; Orlandi, M.; Berardi, S.; Campagna, S.; Bonchio, M.; Sartorel, A.; Scandola, F. Photoinduced Water Oxidation by a Tetraruthenium Polyoxometalate Catalyst: Ion-pairing and Primary Processes with $Ru(bpy)_3^{2+}$ Photosensitizer. *Inorg. Chem.* **2012**, *51*, 7324–7331;
13. Guo, S.-X.; Liu, Y.; Lee, C.-Y.; Bond, A.M.; Zhang, J.; Geletii, Y.V.; Hill, C.L. Graphene-supported $[\{Ru_4O_4(OH)_2(H_2O)_4\}(\gamma\text{-}SiW_{10}O_{36})_2]^{10-}$ for highly efficient electrocatalytic water oxidation, *Energy Environ. Sci.* **2013**, *6*, 2654–2663.
14. Liu, Y.; Guo, S.-X.; Bond, A.M.; Zhang, J.; Geletii, Y.V.; Hill, C.L. Voltammetric Determination of the Reversible Potentials for $[\{Ru_4O_4(OH)_2(H_2O)_4\}(\gamma\text{-}SiW_{10}O_{36})_2]^{10-}$ over the pH Range of 2-12: Electrolyte Dependence and Implications for Water Oxidation Catalysis, *Inorg Chem* **2013**, *52*, 11986–11996.
15. Anwar, N.; Sartorel, A.; Yaqub, M.; Wearen, K.; Laffir, F.; Armstrong, G.; Dickinson, C.; Bonchio, M.; McCormac, T. Surface immobilization of a tetra-ruthenium substituted polyoxometalate water oxidation catalyst through the employment of conducting polypyrrole and the layer-by-layer (LBL) technique, *ACS Appl. Mater. Interfaces* **2014**, *6*, 8022–8031.
16. Hill, C.L. POMs in Catalysis. *J. Mol. Catal. A* **2007**, 262 1-242.

17. Kholdeeva, O.A.; Maksimchuk N.V.; Maksimov, G.M. Polyoxometalate-based heterogeneous catalysts for liquid phase selective oxidations: Comparison of different strategies. *Catal. Today* **2010**, *157*, 107–113.
18. Mizuno, N.; Kamata K.; Yamaguchi, K. Green Oxidation Reactions by Polyoxometalate-Based Catalysts: From Molecular to Solid Catalysts. *Top. Catal.* **2010**, *53*, 876–893.
19. Neumann, R. Activation of Molecular Oxygen, Polyoxometalates, and Liquid-Phase Catalytic Oxidation, *Inorg. Chem.* **2010**, *49*, 3594–3601.
20. Han,; Z.G. Bond A.M.; Zhao, C. Recent trends in the use of polyoxometalate-based material for efficient water oxidation. *Sci. China Chem.* **2011**, *54*, 1877–1887.
21. Maksimchuk, N.V.; Kholdeeva, O.A.; Kovalenko, K.A.; Fedin, V.P. MIL-101 Supported Polyoxometalates: Synthesis, Characterization, and Catalytic Applications in Selective Liquid-Phase Oxidation. *Isr. J. Chem.* **2011**, *51*, 281–289.
22. Mizuno N.; Kamata, K. Catalytic oxidation of hydrocarbons with hydrogen peroxide by vanadium-based polyoxometalates. *Coord. Chem. Rev.* **2011**, *255*, 2358–2370.
23. Deng, W.; Zhang Q.; Wang, Y. Polyoxometalates as efficient catalysts for transformations of cellulose into platform chemicals. *Dalton Trans.* **2012**, *41*, 9817–9831.
24. Lv, H.; Geletii, Y.V.; Zhao, C.; Vickers, J.W.; Zhu, G.; Luo, Z.; Song, J.; Lian, T.; Musaev D.G.; Hill, C.L. Polyoxometalate water oxidation catalysts and the production of green fuel. *Chem. Soc. Rev.* **2011**, *41*, 7572–7589.
25. Stracke, J.J.; Finke, R.G. Distinguishing Homogeneous from Heterogeneous Water Oxidation Catalysis when Beginning with Polyoxometalates, *ACS Catal.* **2014**, *4*, 909–933.
26. Sumliner, J.M.; Lv, H.; Fielden, J.; Geletii, Y.V.; Hill, C.L. Polyoxometalate Multi-Electron-Transfer Catalytic Systems for Water Splitting, *Eur. J. Inorg. Chem.* **2014**, 635–644.
27. Himeno, S.; Saito, A. Preparation of dodecamolybdovanadate(V). *Inorg. Chim. Acta* **1990**, *171*, 135–137.
28. Himeno, S.; Takamoto, M.; Higuchi, A.; Maekawa, M. Preparation and voltammetric characterization of Keggin-type tungstovanadate $[VW_{12}O_{40}]^{3-}$ and $[V(VW_{11})O_{40}]^{4-}$ complexes. *Inorg. Chim. Acta* **2003**, *348*, 57–62.
29. Himeno, S.; Kawasaki, K.; Hashimoto, M. Preparation and characterization of an α-Wells-Dawson-type $[V_2Mo_{18}O_{62}]^{6-}$ complex. *Bull. Chem. Soc. Jpn.* **2008**, *81*, 1465–1471.
30. Miras, H.N.; Ochoa, M.N. C.; Long, D.-L.; Cronin, L. Controlling transformations in the assembly of polyoxometalate clusters: $\{Mo_{11}V_7\}$, $\{Mo_{17}V_8\}$ and $\{Mo_{72}V_{30}\}$, *Chem. Commun.* **2010**, *46*, 8148–8150.
31. Miras, H.N.; Stone, D.; Long, D.-L.; McInnes, E.J. L.; Kogerler, P.; Cronin, L. Exploring the Structure and Properties of Transition Metal Templated $\{VM_{17}(VO_4)_2\}$ Dawson-Like Capsules, *Inorg. Chem.* **2011**, *50*, 8384–8391.
32. Miras, H.N.; Sorus, M.; Hawkett, J.; Sells, D.O.; McInnes, E.J. L.; Cronin, L. Oscillatory Template Exchange in Polyoxometalate Capsules: A Ligand-Triggered, Redox-Powered, Chemically Damped Oscillation. *J. Am. Chem. Soc.* **2012**, *134*, 6980–6983.
33. Pettersson, L.; Andersson, I.; Oehman, L.O. Multicomponent polyanions. 35. A phosphorus-31 NMR study of aqueous molybdophosphates. *Acta Chem. Scand., Ser. A* **1985**, *A39*, 53–58.

34. Pettersson, L.; Andersson, I.; Oehman, L.O. Multicomponent polyanions. 39. Speciation in the aqueous hydrogen ion-molybdate(MoO_4^{2-})-hydrogenphosphate(HPO_4^{2-}) system as deduced from a combined Emf-phosphorus-31 NMR study. *Inorg. Chem.* **1986**, *25*, 4726–4733.
35. Pettersson, L.; Andersson, I.; Grate, J.H.; Selling, A. Multicomponent Polyanions. 46. Characterization of the Isomeric Keggin Decamolybdodivanadophosphate Ions in Aqueous Solution by ^{31}P and ^{51}V NMR. *Inorg. Chem.* **1994**, *33*, 982–993.
36. Katano, H.; Osakai, T.; Himeno, S.; Saito, A. A kinetic study of the formation of 12-molybdosilicate and 12-molybdogermanate in aqueous solutions by ion transfer voltammetry with the nitrobenzene-water interface. *Electrochim. Acta* **1995**, *40*, 2935–2942.
37. Ueda, T.; Sano, K.; Himeno, S.; Hori, T. Formation and conversion of yellow molybdophosphonate complexes in aqueous-organic media. *Bull. Chem. Soc. Jpn.* **1997**, *70*, 1093–1099.
38. Himeno, S.; Ueda, T.; Shiomi, M.; Hori, T. Raman studies on the formation of 12-molybdopyrophosphate. *Inorg. Chim. Acta* **1997**, *262*, 219–223.
39. Himeno, S.; Sano, K.; Niiya, H.; Yamazaki, Y.; Ueda, T.; Hori, T. Formation and conversion of yellow heteropoly complexes in a Mo(VI)-Se(IV), Te(IV) system, *Inorg. Chim. Acta* **1998**, *281*, 214–220.
40. Selling, A.; Andersson, I.; Grate, J.H.; Pettersson, L. Multicomponent polyanions. 49. A potentiometric and (^{31}P, ^{51}V) NMR study of the aqueous molybdovanadophosphate system. *Eur. J. Inorg. Chem.* **2000**, 1509–1521.
41. Himeno, S.; Takamoto, M.; Ueda, T. Formation of α- and β-Keggin-Type $[PW_{12}O_{40}]^{3-}$ Complexes in Aqueous Media, *Bull. Chem. Soc. Jpn.* **2005**, *78*, 1463–1468.
42. Hashimoto, M.; Andersson, I.; Pettersson, L. An equilibrium analysis of the aqueous H^+-MoO_4^{2-}-$(HP)O_3^{2-}$ and H^+-MoO_4^{2-}-$(HP)O_3^{2-}$-HPO_4^{2-} systems. *Dalton Trans.* **2007**, 124–132.
43. Hashimoto, M.; Andersson, I.; Pettersson, L. A ^{31}P-NMR study of the H^+-$MoO4^{2-}$-$(HP)O_3^{2-}$-HPO_4^{2-}-$(C_6H_5P)O_3^{2-}$-$(CH_3P)O_3^{2-}$ system at low Mo_{tot}/P_{tot} ratio - Formation of mixed-hetero X_2M_5-type polyanions. *Dalton Trans.* **2009**, 3321–3327.
44. Ueda, T.; Wada, K.; Hojo, M. Voltammetric and Raman spectroscopic study on the formation of Keggin-type V(V)-substituted molybdoarsenate complexes in aqueous and aqueous-organic solution, *Polyhedron* **2001**, *20*, 83–89.
45. Ueda, T.; Nambu, J.; Yokota, H.; Hojo, M. The effect of water-miscible organic solvents on the substitution reaction of Keggin-type heteropolysilicates and -germanates with vanadium(V) ion. *Polyhedron* **2009**, *28*, 43–48.
46. Ueda, T.; Ohnishi, M.; Shiro, M.; Nambu, J.-i.; Yonemura, T.; Boas, J.F.; Bond, A.M. Synthesis and Characterization of Novel Wells-Dawson-Type Mono Vanadium(V)-Substituted Tungsto-polyoxometalate Isomers: 1- and 4-$[S_2VW_{17}O_{62}]^{5-}$. *Inorg. Chem.* **2014**, *53*, 4891–4898.
47. Himeno, S.; Hashimoto, M.; Ueda, T. Formation and conversion of molybdophosphate and -arsenate complexes in aqueous solution. *Inorg. Chim. Acta* **1999**, *284*, 237–245
48. Roy, S.K.; Day, K.C. Synthesis and characterization of sodium, potassium, guanidinium and tetramethylammonium salts of 17-tungstovanadodiarsenate(V). *Ind. J. Chem.* **1992**, 31A, 64–66.
49. Contant, R.; Abbessi, M.; Thouvenot, R.; Herve, G. Dawson Type Heteropolyanions. 3. Syntheses and ^{31}P, ^{51}V, and ^{183}W NMR Structural Investigation of Octadeca(molybdotungstovanado) diphosphates Related to the $[H_2P_2W_{12}O_{48}]^{12-}$ Anion. *Inorg. Chem.* **2004**, *43*, 3597–3604.

50. Contant, R.; Klemperer, W. G.; Yaghi, O. Potassium Octadecatungstodiphosphates(V) and Related Lacunary Compounds. *Inorg. Synth.* **1990**, *27*, 104–111.
51. Rob van Veen, J.A.; Sudmeijer, O.; Emeis, C.A.; Wit, H. On the identification of molybdophosphate complexes in aqueous solution. *Dalton Trans.* **1986**, 1825–1831.
52. Rocchiccioli-Deltcheff, C.; Fournier, M.; Franck, R.; Thouvenot, R. Vibrational investigations of polyoxometalates. 2. Evidence for anion-anion interactions in molybdenum(VI) and tungsten(VI) compounds related to the Keggin structure. *Inorg. Chem.* **1983**, *22*, 207–216.
53. Contant, R.; Thouvenot, R. Hétéropolyanions de type Dawson. 2. Synthèses de polyoxotungstoarsénates lacunaires dérivant de l'octadécatungstodiarsénate. Étude structurale par RMN du tungstène-183 des octadéca(molybdotungstovanado)diarsénates apparentés. *Can. J. Chem.* **1991**, *69*, 1498–1506 (In French).
54. Abbessi, M.; Contant, R.; Thouvenot, R.; Herve, G. Dawson type heteropolyanions. 1. Multinuclear (phosphorus-31, vanadium-51, tungsten-183) NMR structural investigations of octadeca(molybdotungstovanado)diphosphates .alpha.-1,2,3-$[P_2MM'_2W_{15}O_{62}]^{n-}$ (M, M' = Mo, V, W): syntheses of new related compounds. *Inorg. Chem.* **1991**, *30*, 1695.
55. Pope, M.T. Heteropoly and isopoly anions as oxo complexes and their reducibility to mixed-valence blues. *Inorg. Chem.* **1972**, *11*, 1973–1974.
56. Smith, D.P.; Pope, M.T. Heteropoly 12-metallophosphates containing tungsten and vanadium. Preparation, voltammetry, and properties of mono-, di-, tetra-, and hexavanado complexes. *Inorg. Chem.* **1973**, *12*, 331–336.
57. Altenau, J.J.; Pope, M.T.; Prados, R.A.; So, H. Models for heteropoly blues. Degrees of valence trapping in vanadium(IV)- and molybdenum(V)-substituted Keggin anions. *Inorg. Chem.* **1975**, *14*, 417–421.
58. Himeno, S.; Osakai, T.; Saito, A. Preparation and Properties of Heteropoly Molybdovanadate(V) Complexes. *Bull. Chem. Soc. Jpn.* **1991**, *64*, 21–28.